Bone 155 (2022) 116299

Contents lists available at ScienceDirect

Bone

journal homepage: www.elsevier.com/locate/bone

Glucocorticoid caused lactic acid accumulation and damage in human chondrocytes via ROS-mediated inhibition of Monocarboxylate Transporter 4

Qingxian Li [1], Haitao Chen [1], Zhenyu Li, Fan Zhang, Liaobin Chen [*]

Division of Joint Surgery and Sports Medicine, Department of Orthopedic Surgery, Zhongnan Hospital of Wuhan University, Wuhan 430071, China

ARTICLE INFO

Keywords:
Dexamethasone
Cartilage
Reactive oxygen species
Monocarboxylate transporter 4
Lactic acid
H3K4me3

ABSTRACT

Osteoarthritis (OA) is a common joint disease lacking effective treatments. Dexamethasone (Dex) is often used to relieve joint pain. However, the adverse effects of Dex on cartilage can't be ignored. This study aimed to investigate the effect of Dex on articular cartilage and its mechanism by in vitro and in vivo experiments. The results showed that intra-articular injection with Dex damaged the matrix synthesis of cartilage. In vitro, Dex induced human chondrocytes mitochondrial dysfunction and increased reactive oxygen species (ROS) level, while down-regulated or unchanged key glycolysis genes, but increased lactic acid (LA) concentration. It was showed that high concentrations of LA induced chondrocytes apoptosis. Mechanistically, monocarboxylate transporter 4 (MCT4) was inhibited by Dex and had a significant negative correlation with ROS level. Further results showed that the trimethyl-histone H3-K4 (H3K4me3) level of MCT4 was reduced by Dex, and the ROS scavenger N-Acetyl-L-cysteine (NAC) and α-ketoglutarate (α-KG) alleviated the Dex-induced obstruction of matrix synthesis and high level of ROS by up-regulating the H3K4me3 level of MCT4 and its expression. In conclusion, Dex exhibited harm to cartilage, shown as mitochondrial dysfunction and increased ROS. The latter further caused LA accumulation in chondrocytes via decreasing the H3K4me3 level of MCT4 and its expression, which may account for the long-term side effects of Dex on chondrocytes. And α-KG may be used as an auxiliary drug to weaken the toxic effect of Dex on cartilage.

1. Introduction

Osteoarthritis (OA) is one of the common age-related arthritis and is characterized by cartilage degradation [1,2]. Meanwhile, OA is a major source of pain, disability, as well as socioeconomic cost worldwide [3]. Currently, no proven disease-modifying medications are available for OA, and all the conservative treatments are mostly symptomatic. Intra-articular (IA) injections with glucocorticoids (GCs) are widely used to combat joint pain and inflammation and are recommended treatment modalities of knee OA [1,4]. IA GCs had great benefits for pain relief [5,6], but it is also reported that IA GCs caused significantly greater cartilage volume loss [7] and adverse structural effects [8].

Dexamethasone (Dex) is one kind of GCs with wider clinical application, especially used to suppress inflammation [1]. Pemmari et al. [9] demonstrated the anti-inflammatory and anticatabolic effect of Dex on chondrocytes. However, the clinical application of Dex should be

Abbreviations: 18S, 18S ribosomal RNA; Acan, aggrecan; Adamts5, ADAM metallopeptidase with thrombospondin type 1 motif 5; ATP (6, 8), mitochondrially encoded ATP synthase membrane subunit (6, 8); ChIP, chromatin immunoprecipitation; Col2a1, α1 chain of type II collagen gene; COX (1–3), mitochondrially encoded cytochrome C oxidase (1–3); Dex, dexamethasone; ECM, extracellular matrix; GAG, glycosaminoglycan; Gapdh, glyceraldehyde phosphate dehydrogenase; GCs, glucocorticoids; H_2O_2, hydrogen peroxide; H3K4me3, trimethyl-histone H3-K4; Hk1, hexokinase 1; IA, intra-articular; IF, immunofluorescence; IHC, immunohistochemical; IOD, integrated optical density; LA, lactic acid; LDH, lactate dehydrogenase; MCT4, monocarboxylate transporter 4; Mito, mitochondrion; Mmp3, matrix metallopeptidase 3; mtDNA, mitochondrial DNA; NAC, N-Acetyl-L-cysteine; ND (1–5), mitochondrially encoded NADH dehydrogenase (1–5); OA, osteoarthritis; OXPHOS, oxidative phosphorylation; Pfkm, phosphofructokinase; Pkm, pyruvate kinase; ROS, reactive oxygen species; SA-β-Gal, senescence-associated β-galactosidase; TEM, transmission electron microscopy; α-KG, α-ketoglutarate; ΔΨm, mitochondrial membrane potential.

* Corresponding author at: Division of Joint Surgery and Sports Medicine, Department of Orthopedic Surgery, Zhongnan Hospital of Wuhan University, Wuhan 430071, China.

E-mail address: lbchen@whu.edu.cn (L. Chen).

[1] Qingxian Li and Haitao Chen have contributed equally to this work.

https://doi.org/10.1016/j.bone.2021.116299
Received 8 September 2021; Received in revised form 23 November 2021; Accepted 9 December 2021
Available online 13 December 2021

cautious considering its potential long-term side effects, including weight gain, poor wound healing, avascular necrosis of the femoral head, osteoporosis, and so on [10]. Tu et al. [11] have reported the toxic effects of Dex on chondrocyte viability through increasing apoptosis and inhibiting proliferation. Also, several lines of investigation have demonstrated that corticosteroids have long-term deleterious effects on cartilage [7,12,13]. However, the specific mechanism underlying the harm of Dex to cartilage remained unclear.

Mitochondria play an important role in maintaining chondrocyte homeostasis [14]. Oxidative phosphorylation (OXPHOS) takes place at the inner mitochondrial membrane and is an efficient form for ATP production [15]. It is reported that articular chondrocytes possess mitochondrial respiration in vitro, and OXPHOS may account for 25% of total steady-state ATP production [16,17]. At rest, the synovial joint is a relatively hypoxic environment, and chondrocytes rely primarily on glycolysis to meet cellular energy needs [17,18]. The process of glycolysis may result in high levels of lactic acid (LA) production. To maintain a normal intracellular pH, the LA transport, named monocarboxylate transporter 4 (MCT4) carries out a crucial role in transporting LA out of the cell [19]. Chondrocyte metabolic flexibility promotes cell survival during multiple environmental stress, and chondrocytes adapt their metabolism to microenvironmental changes by shifting the metabolic pathways [2,18]. Recently, Dex was reported to be associated with abnormal respiratory metabolism based on RNA sequences [9,20]. However, the specific role of Dex in respiratory metabolism is worthy of further study.

This study aimed to study the effect of Dex on cartilage considering the respiratory metabolism changes of chondrocytes. Besides, this study will explore how Dex causes a long-lasting impact on cartilage after the application of Dex.

2. Materials and methods

2.1. Chemicals and reagents

Dex (No. H42020019) was purchased from Shuanghe Pharmaceutical Company (Wuhan, China). TRIzol (SKU: R6830-02) was purchased from Invitrogen (Carlsbad, CA, USA). Collagenase II (No. 17101015), foetal bovine serum (FBS) (No. 16000-044), and DMEM/F12 medium (No. 11330032) were purchased from Gibco (Grand Island, NY, USA). Triton X-100 (No. T8532) was purchased from Sigma (St. Louis, MO, USA). Reverse transcription and real-time quantitative polymerase chain reaction (RT-qPCR) kits were purchased from Takara Biotechnology (Dalian, China), SYBR green dye was purchased from Applied Biosystems, by Thermo Fisher Scientific (ABI) (Foster City, CA, USA). Safranin O (CAS No. 477-73-6) and Fast Green (CAS No. 2353-45-9) were obtained from Hengyuan Biotech (Shanghai, China). Senescence β-Galactosidase staining kit (No. C0602), 4′,6-diamidino-2-phenylindole (DAPI) (No. C1002), mitochondrial membrane potential assay kit with JC-1 (No. C2006), cell counting kit-8 (CCK-8) (No. C0038), Hoechst 33342 staining solution (No. C1027), RIPA lysis buffer (No. P0013B), BCA protein assay kit (No. P0012S) and reactive oxygen species (ROS) assay kit (No. S0033S) were obtained from Beyotime Biotech Inc. (Shanghai, China). Blood & Cell culture DNA mini kit (No. 13323) was purchased from Qiagen Co., Ltd. (Shanghai, China). LA assay kit (No. A019-2-1) and lactate dehydrogenase (LDH) assay kit (No. A020-2) were obtained from Nanjing Jiancheng Bioengineering Institute (Nanjing, China). DL-LA (No. MB2836) was purchased from Meilun Biotechnology Co., Ltd. (Dalian, China). Dimethyl 2-oxoglutarate (dimethyl-α-ketoglutarate, α-KG) (CAS No.13192-04-6) was purchased from Sigma (St. Louis, MO, USA). N-Acetyl-L-cysteine (NAC) (CAS No. 616-91-1) were obtained from MedChemExpress LLC (Shanghai, China). All primers were synthesized by Sangon (Shanghai, China). Polyclonal antibody rabbit anti-MCT4 (No. bs-2698R) was acquired from Beijing Biosynthesis Biotechnology Co., Ltd. (Beijing, China), anti-trimethyl-histone H3-K4 rabbit pAb (H3K4me3) (No. A2357), anti-α1 chain of type II collagen gene (COL2A1) rabbit pAb (A1560) were acquired from ABclonal Technology Co., Ltd. (Wuhan, China). Anti-aggrecan (ACAN) (No. 13880–1-AP) was obtained from Proteintech Group, Inc. (Wuhan, China). The secondary antibody information is as follows: goat anti-rabbit and horseradish peroxidase-conjugated IgG (No. 4412) was obtained from Cell Signaling Technology (Danvers, MA, USA); Cy3 conjugated goat anti-rabbit IgG (H + L) (No. AS-1111) was obtained from ABclonal (Wuhan, China). The other reagents used for the experiments were of analytical grade.

2.2. Animals and treatment

Specific pathogen-free male Wistar rats (No. 2015–2018, certification number: 42000600014526, license number: SCXK) (Hubei, China) weighing 260 ± 20 g (7 weeks old), were obtained from the Experimental Center of the Hubei Medical Scientific Academy (Wuhan, China). All animal experimental procedures were conducted by the Guidelines for the Care and Use of Laboratory Animals of the Chinese Animal Welfare Committee. The program was approved by the Animal Experimental Ethics Committee of Wuhan University Medical College (license number: 14016).

The animal treatment was performed as described before [21]. Briefly, animals were acclimated 1 week before experimentation. In this study, rats were divided into the control group (saline-treated) and the Dex group (Dex-treated) ($n = 8$/group). The left and right knees of rats in the Dex group were intra-articularly injected with Dex (dissolved in saline, 0.5 mg/kg, 10 μL each time) twice per week, and that in the control group were given an equal volume of saline twice per week. The dose chosen of Dex was referred to clinic practice [22–24]. All rats were sacrificed after being anesthetized with 2–3% isoflurane after 8 weeks of treatment, and the rat's joint tissues were harvested for histological staining and gene analysis. The left joints were embedded in wax blocks for histological staining and analysis ($n = 8$), and the right joints were used for gene analysis ($n = 8$).

2.3. Resource and culture of primary human chondrocytes

The chondrocytes used in the in vitro experiments were derived from human cartilage. The protocol used in this study complies with the ethical guidelines of the Helsinki Declaration in 1975 and was approved by the Medical Ethics Committee Zhongnan Hospital, Wuhan University (No. 2019018). The patient's written informed consent was obtained for all operations involved. Three cartilage tissue was collected from three male patients who underwent total knee arthroplasty (TKA) surgery (aged between 50 and 70 years old), and chondrocytes derived from an unabraded area in the articular cartilage. Cartilage was fully chopped under sterile conditions, digested with 0.2% type II collagenase solution at 37 °C for 6–8 h, centrifuged at 120 ×g for 5 min, and then resuspended in F12 medium containing 10% fetal calf serum. Primary cells were seeded at a density of 2.0×10^2 cells/mm^2. The chondrocytes were cultured with an F12 medium containing 10% FBS. Then, 100 U/mL penicillin and 50 μg/mL streptomycin were added to the above culture system. 0.25% trypsin was used to sub-culture cells. Subsequent experiments were performed after two generations. When the cells reached 80% confluence, different concentrations of Dex dissolved in DMSO were added to six-well plates (the final concentration of DMSO was 0.1%), and the same volume of control medium containing 0.1% DMSO was added to the control cells. For in vitro experiments, n values represented the number of independent experiments or the number of cell samples detected. For each independent experiment, at least three technical replicates were used.

2.4. Total RNA extraction and real-time qPCR (RT-qPCR)

Total RNA was isolated using TRIzol reagent following the manufacturer's protocol. An Applied Biosystems TaqMan Reverse

Transcription kit was used to convert mRNA to cDNA. RT-qPCR was then performed using a SYBR Green qPCR Master Mix Kit and an ABI Step One Plus cycler (Applied Biosystems, Foster City, CA, USA) at 95 °C for 40 cycles of 15 s and 60 °C for 30 s. The gene expression relative to the expression of GAPDH was calculated by the $2^{-\Delta\Delta CT}$ method for standardization. The primer sequences and annealing temperatures are shown in Table 1.

2.5. Mitochondrial DNA (mtDNA) copy number

Relative mitochondrial copy number detection referred to a previous study [25]. Briefly, the total DNA of chondrocytes was extracted using a DNA extraction kit. Primer sequences for the mitochondrial segment *ND1(DNA)* and single-copy nuclear contral *18S (DNA)* were shown in Table 1. The relative mitochondrial copy number was calculated using the following equations: ΔC_T = mitochondrial C_T - nuclear C_T, relative mitochondrial DNA content = $2 \times 2^{-\Delta CT}$.

2.6. Cellular immunofluorescence (IF) staining

Chondrocytes were cultured in confocal dishes, and were washed with PBS and fixed with 4% paraformaldehyde for 15 min. The cells were blocked with 3% BSA in PBS for 60 min at 4 °C. Primary antibody anti-MCT4 (1: 200 dilution) was added and incubated overnight at 4 °C. Fluorescent secondary antibody (1:100) was added for 2 h at 25 °C, -incubated with DAPI for 5 min at 25 °C, and observed using a confocal microscope (Leica-LCS-SP8-STED, Leica, Germany). The intensity of the staining was determined by measuring the mean integrated optical density (IOD) of per cell in 10 different fields of view for each sample.

2.7. Immunohistochemical (IHC) staining

IHC was performed as described before [26]. Briefly, the fixed tissues were put into the EDTA decalcification fluid (Servicebio technology CO., LTD, Wuhan, China) for slow decalcification at room temperature. The degree of decalcification is observed every 2 days. After the tissue is completely softened, the next step of embedding and slicing is carried out. The knees of the rats were sectioned sagittally at 4 μm for morphological staining analysis. BSA was used to block the previously added primary antibody anti-MCT4 (1:200 dilution). Then, a DAB staining kit (GeneTech Company, Ltd., Shanghai, China) was used for the protein expression of MCT4 in articular cartilage. All of the images were captured and then analyzed using a Nikon NIS Elements BR light microscope (Nikon, Tokyo, Japan). To quantify the protein expression of MCT4 in cartilage, the staining intensity was determined by measuring the immunoreactive score (IRS) as described previously [27]. Briefly, five different fields were observed and 100 cells were counted for each sample, and immunoreaction was divided into five grades depending on the percentage of positive cells (percentage scores): <10% (0), 10–25% (1), 25–50% (2), 50–75% (3), and >75% (4). The intensity of staining was divided into four grades (intensity scores): no staining (0), light brown (1), brown (2), and dark brown (3). Scoring formula: IRS = percentage score × intensity score.

Table 1
Oligonucleotide primers and PCR conditions in real-time quantitative PCR.

Genes	Forward primer	Reverse primer
Gapdh (human)	GTCAGTGGTGGACCTGACCT	TGCTGTAGCCAAATTCGTTG
Gapdh (rat)	TAAAGAACAGGCTCTTAGCACA	AGTCTTGGAAATGGATTGTCTC
Col2a1 (human)	ACGGGTGAACCTGGTATT	CACCTGTCTCACCATCTTTG
Col2a1 (rat)	GAGGGCAACAGCAGGTTCAC	GCCCTATGTCCACACCAAATTC
Acan (human)	GGTTGAGAATGAGACTGGAGAG	GTCTGGTTAGGGTAGAGGTAGA
Acan (rat)	TGGCATTGAGGACAGCGAAG	TCCAGTGTGTAGCGTGTGGAAATAG
Mmp3 (human)	TCTCTTTCACTCAGCCAACAC	GTATCCAGCTCGTACCTCATTTC
Mmp3 (rat)	CTCGAACACTATGGAGCTGATG	AGGTCTGTGGAGGACTTGTA
Mmp13 (human)	GACCCTTCCTTATCCCTTGATG	CATATCTCCAGACCTGGTTTCC
Mmp13 (rat)	TGACCTGGGATTTCCAAAAGAG	GTCTTCCCCGTGTCCTCAAA
Adamts4 (human)	TCCCATGTGCAACGTCAA	GAGCCTCTGGTTTGTCTAAGAG
Adamts4 (rat)	TCGCTTCGCTGAGTAGATTCGT	TTCGGATGCTTGGATGCTTAA
Adamts5 (human)	GCACTGGCTACTATGTGGTATT	TCTAGTCTGGTCTTTGGCTTTG
Adamts5 (rat)	GCAACAAAGTGGGACTACA	GAGAGAATGCATCCCTTAGC
Hk1 (human)	CTCCTGCATCTCTGACTTCTTG	CCATCTCCACGTTCTTCATCTC
Hk1 (rat)	CATGATGACCTGTGCGTATGA	CTCCACCATCTCCACATTCTTC
Pfkm (human)	GTGGCTCTAAACTTGGGACTAAA	GTTGGAGACTGTAGCAGGAATG
Pfkm (rat)	TCTGGCCAAAGGTCAGATTG	GTTCCAGGTTCTTCTTGGGTAG
Pkm (human)	GGGAGAGAAGGGAAAGAACATC	TCAGCACAATGACCACATCTC
Pkm (rat)	GAAGGAGAAAGGTGCTGACTAC	TTACACAGCACAGGGAAGATG
Mct1 (rat)	CTTGTCCCTGTTTACCCATAGAG	GAGCCAACCAAAGGCAAATC
Mct4 (human)	TTCGTCATCACTGGCTTCTC	TGAAGAGGTAGACGGAGTAGG
Mct4 (rat)	CATAACAGGGCTCAAGAAGG	CCATACGAGATCCCAAAGAAG
ND1 (human)	CGATTCCGCTACGACCAACT	AGGTTTGAGGGGGAATGCTG
ND2 (human)	AGCACCACGACCCTACTACT	TGGTGGGGATGATGAGGCTA
ND3 (human)	GCGGCTTCGACCCTATATCC	AGGGCTCATGGTAGGGGTAA
ND4 (human)	GCTCCATCTGCCTACGACAA	GCTTCAGGGGGTTTGGATGA
ND5 (human)	CACACCGCACAATCCCCTAT	TGGAGGTGGAGATTTGGTGC
COX1 (human)	TTAGCTGACTCGCCACACTC	AGTGGAAGTGGGCTACAACG
COX2 (human)	GTACTCCCGATTGAAGCCCC	ACCGTAGTATACCCCCGGTC
COX3 (human)	ACCCTCCTACAAGCCTCAGA	TGACGTGAAGTCCGTGGAAG
ATP6 (human)	ACCACAAGGCACACCTACAC	TATTGCTAGGGTGGCGCTTC
ATP8 (human)	ATACTACCGTATGGCCCACC	GGGCTTTGGTGAGGGAGGTA
ND1(DNA) (human)	CCTTTAACCTCTCCACCCTTATC	GAGGTGTATGAGTTGGTCGTAG
18S (DNA) (human)	CCCAACTTCTTAGAGGGACAAG	GTACAAAGGGCAGGGACTTAAT

Gapdh: glyceraldehyde phosphate dehydrogenase; *Col2a1*: α1 chain of type II collagen gene; *Acan:* aggrecan; *Mmp (3,13):* matrix metallopeptidase (3, 13); *Adamts(4, 5):* ADAM metallopeptidase with thrombospondin type 1 motif (4, 5); *Hk1:* hexokinase 1; *Pfkm*: phosphofructokinase; *Pkm:* pyruvate kinase; *Mct (1, 4):* monocarboxylate transporter (1, 4); *ND (1–5):* mitochondrially encoded NADH dehydrogenase (1–5); *COX (1–3):* mitochondrially encoded cytochrome C oxidase (1–3); *ATP (6, 8):* mitochondrially encoded ATP synthase membrane subunit (6, 8); *18S:* 18S ribosomal RNA.

2.8. Electron microscopic examination

The experiment was performed as described before [28]. Briefly, chondrocytes were collected after the treatment of Dex and were fixed with electromicroscope fixative. Ultrathin sections (~50 nm) were cut with LKB-Vultra microtome (Bromma, Sweden), stained with uranyl acetate and lead citrate, and examined with a Hitachi H600 transmission electron microscope (Hitachi, Tokyo, Japan). Choosing 5 fields of view for each sample, and then selecting a representative image in each group for analysis.

2.9. Safranin O and Fast Green staining

Safranin O and Fast Green staining was performed as described before [26]. Briefly, the knees of the rats were sectioned sagittally at 4 μm. Then, the slices were stained with Fast Green for 5–10 min and then washed with water, and quickly dehydrated with absolute ethanol after staining Safranin O for 15–30 s. Clear xylene was applied to transparent sections for 5 min, and they were sealed with neutral gum. For chondrocyte Safranin O staining, rinsed with PBS for 3 times, fixed with 4% paraformaldehyde for 15 min, and then stained with Safranin O for 1–2 min. Finally, we observed and took pictures under the microscope.

All of the images were captured and then were analyzed using a Nikon NIS Elements BR light microscope (Nikon, Tokyo, Japan). The staining intensity was determined by measuring the IOD in 10 different fields for each sample via Image J software (National Institutes of Health, Bethesda, MD, USA).

2.10. Senescence-associated β-galactosidase (SA-β-Gal) staining

Cellular senescence was assessed by detecting the activity of β-galactosidase using an SA-β-gal staining kit (Beyotime) according to the manufacturer's instructions. Briefly, cultured cells in 6-well plates were immersed in a fixative solution for 15 min at room temperature. After rinsing with PBS, cells were incubated with freshly prepared staining work solution overnight at 37 °C. All the images were captured and then were analyzed using a Nikon NIS Elements BR light microscope (Nikon, Tokyo, Japan). The percentage of positive cells was analyzed in 10 different fields for each sample.

2.11. JC-1 assay for mitochondrial membrane potential (ΔΨm)

The JC-1 probe was used to detect the ΔΨm of chondrocytes. According to the manufacturer's instructions (Beyotime), the cells cultured in the confocal dish were incubated with a fresh mixture of 1 mL of DMEM/F12 medium and 1 mL JC-1 dyeing working solution. The images were observed using a laser confocal microscope (Leica-LCS-SP8-STED, Leica, Germany). The relative ratio of red and green fluorescence is a measure of the ratio of mitochondrial depolarization.

2.12. Western blot

RIPA buffer and protease inhibitors were used for total cell protein extraction. Then, total protein was subjected to sodium dodecyl sulfate-polyacrylamide gel electrophoresis (SDS-PAGE) and electrophoretically transferred to PVDF membranes. After blocking with fresh 5% nonfat milk, the blots were incubated with primary antibodies in 5% BSA overnight at 4 °C. Then, the membranes were incubated with anti-rabbit or anti-mouse IgG for 2 h at room temperature. After three washes in TBS, immuno-reactive bands were detected by adding ECL substrate. Image J software (Software Inquiry; Quebec, Canada) was used to quantify the bands. The following primary antibodies were used: MCT4 (1:1000 dilution), COL2A1 (1:1000 dilution), and ACAN (1:1000 dilution).

2.13. Transfection

MCT4 overexpression plasmids were produced by Shanghai GenePharma Co., Ltd. (Shanghai, China). The MCT4 plasmid was constructed based on the CDS (Coding sequence) region. Subconfluent human chondrocytes in 6-well plates were transfected in triplicate with 2.5 μg of MCT4 overexpression plasmid using LipofectamineTM 3000 and P3000TM transfection reagent (Invitrogen, USA) according to the protocol of manufacture. After 1 day and 2 days, human chondrocytes were collected for further analysis of mRNA and protein levels.

2.14. ROS detection

According to the manufacturer's instructions (Beyotime), the cells cultured in the confocal dish were incubated with the DCFH-DA (10 μmol/L) for 20 min in a 37 °C and then were incubated with Hoechst for 5 min at room temperature. The images were observed and collected under a laser confocal microscope (Leica-LCS-SP8-STED, Leica, Germany) using 488 nm excitation wavelength and 525 nm emission wavelength. The intensity of the staining was determined by measuring the mean IOD per cell in 10 different fields of view for each sample.

2.15. CCK-8 Assay

Chondrocytes were seeded into a 96-well plate at a density of 5×10^3 cells per well. On the next day, cells were treated with various concentrations of Dex (0, 250, 500, 1000, 1500, 2000 nM), LA (0, 2.5, 5, 10, 25, 50, 100, 250, 500 mM), NAC (0, 0.5, 1, 2, 5, 10 mM) and α-KG (0, 0.25, 0.5, 1, 2, 5 mM) for 24 and 48 h. After treatment, CCK-8 solution (10 μL) dissolved in 100 μL culture medium was added to each well, and the mixture was incubated for 2–2.5 h at 37 °C. The optical density value was measured at a wavelength of 450 nm using a microplate reader (Bio-Rad, CA, USA). According to the CCK-8 results, we found that the best treatment time (dose) of Dex (0-1000 nM), NAC (5 mM), and α-KG (2 mM) on chondrocytes was 48 h.

2.16. LA concentration and the LDH activity detection

The chondrocytes were cultured in a 12-well plate ($n = 9$), and an equal volume of cell culture medium was added to each well. Different concentrations of Dex were used for 48 h without changing the medium. After the treatment, the concentration of LA and the activity of lactate dehydrogenase in the culture medium and the cells were detected. The cell culture medium was transferred separately into a new EP tube to be tested. Then the cells were rinsed with PBS for 3 times and were lysed with 100ul of RIPA lysis buffer on ice. Next, we transferred the lysis buffer to another batch of EP tubes and used the BCA kit to determine the protein concentration of the cell lysate.

Finally, in the microplate reader, used the absorption light of 530 nm (LA concentration detection) or 450 nm (LDH activity detection) wavelength to detect the absorbance value, and calculated the LA concentration and LDH activity.

2.17. Chromatin immunoprecipitation (ChIP) assay

ChIP-qPCR was performed as described before [26]. Briefly, the cultured chondrocytes were collected, and then the cell lysates DNA was sheered to lengths of approximately 200 base pairs. Then the chromatin was incubated overnight at 4 °C on a nutator/rocker with anti-H3K4me3 and bovine serum albumin-treated protein G beads to reduce the non-specific background binding. The immunoprecipitated DNA-protein complex that was linked to beads was subsequently purified using PCR purification kits. The isolated DNA was then assayed using RT-qPCR. Using standard curves, the input values were compared to the immunoprecipitated samples, with the IgG negative control values subtracted as background. For all of the ChIP experiments, the results were

obtained in 6 independent experiments, and there were 3 repeats within an experiment.

2.18. Statistical analysis

Prism (GraphPad Software, La Jolla, CA, USA, version 8.0) was used for all data analyses. All data values shown were presented as the mean ± S.E.M. Before in vivo experiment, we have calculated that a sample size of 8 rats per group met the requirement of a statistical difference among groups regarding maximal failure load based on a power analysis with $\beta = 0.8$ and $\alpha = 0.05$. For the animal experiments, we used the Mann–Whitney *U* test for comparisons between the control and Dex groups. For in vitro experiments, a one-way analysis of variance (ANOVA) with the Turkey's post-hoc tests for multiple comparisons. Correlation analysis of the mRNA expression of MCT4 with the ROS level was performed using the Pearson correlation coefficient. $P < 0.05$ was considered statistically significant for all of the tests.

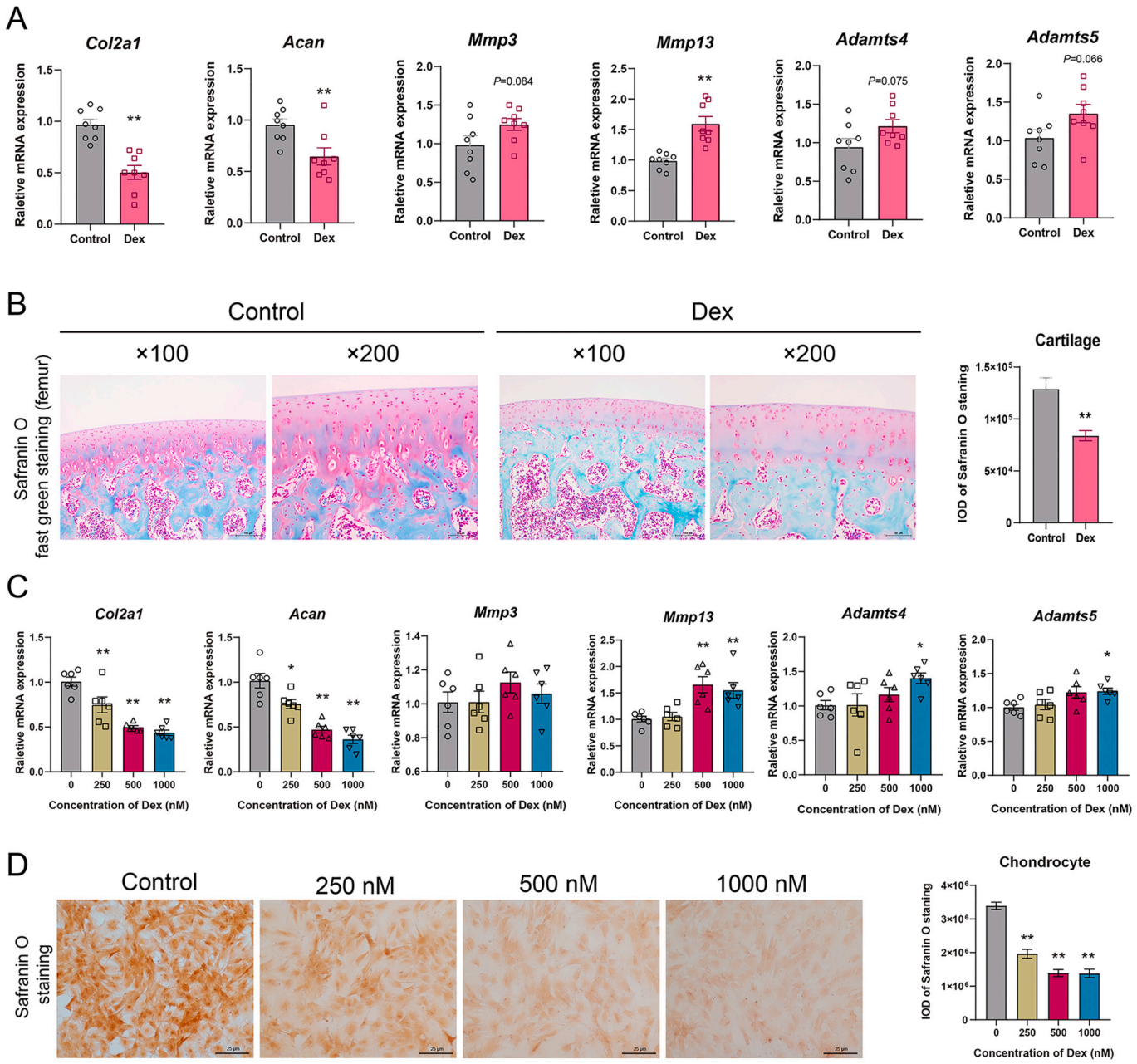

Fig. 1. Dex caused chondrocyte damage. (A) The mRNA expression of α1 chain of type II collagen gene (*Col2a1*), aggrecan (*Acan*), matrix metallopeptidase 3 (*Mmp3*), *Mmp13,* ADAM metallopeptidase with thrombospondin type 1 motif 4 (*Adamts4*) and *Adamts5* in the cartilage of rats, $n = 8$. (B) Representative Safranin O and Fast Green staining images and quantification of the integrated optical density (IOD) of the cartilage (femur) of rats, ×100, ×200, n = 8. (C) The mRNA expression of *Col2a1*, *Acan*, *Mmp3, Mmp13, Adamts4,* and *Adamts5* in human chondrocyte treated with different concentrations of Dex (0 nM, 250 nM, 500 nM, 1000 nM), $n = 6$. (D) Representative Safranin O staining images and quantification of the IOD of human chondrocyte treated with different concentrations of Dex, ×400, $n = 6$. The values are the means ± S.E.M. Mann-Whitney *U* test was used for (A, B) statistical analysis. One-way Anova with Turkey's post hoc tests was used for (C, D) statistical analysis. $^*P < 0.05$, $^{**}P < 0.01$ vs. control. (For interpretation of the references to colour in this figure legend, the reader is referred to the web version of this article.)

3. Results

3.1. Dex damaged the matrix synthesis of chondrocytes

We first observed the effects of Dex on the matrix metabolism of cartilage. RT-qPCR showed that Dex significantly inhibited the mRNA expression of matrix synthesis components (*Col2a1* and *Acan*) but had little influence on the level of matrix-degrading components including *Mmp3*, *Adamts4*, and *Adamts5*, except for increasing the mRNA expression of *Mmp13* (Fig. 1A). Also, Safranin O and Fast Green staining showed extracellular matrix (ECM) loss of cartilage of femur in the Dex group, and quantitative analysis indicated that the Dex group significantly lowered the content of glycosaminoglycan (GAG) (Fig. 1B). Stain in the cartilage of tibia showed the same result (Supplementary Fig. 1A). CCK-8 assay analysis showed that cell viabilities of human chondrocytes were significantly influenced by Dex only when concentrations rose to 1500 nM for 48 h or 500 nM for 72 h (Supplementary Fig. 1B). Therefore, we treated human chondrocytes with Dex at different concentrations (0, 250, 500, and 1000 nM) for 48 h in subsequent experiments. It is shown that Dex decreased the expression of *Col2a1* and *Acan* in a concentration-dependent manner but increased the expression of *Mmp13*, *Adamts 4*, and *Adamts 5* at the concentration of 1000 nM (Fig. 1C). Furthermore, Safranin O staining and SA-β-Gal staining showed that Dex led to more ECM loss (Fig. 1D) and chondrocytes senescence as the concentration of Dex increased (Supplementary Fig. 1C, D). Taken together, our results indicated that Dex can damage the matrix synthesis of chondrocytes and may promote chondrocytes senescence.

3.2. Dex led to mitochondrial dysfunction and increased level of ROS

To further explore the mechanism underlying damaged matrix synthesis, we examined the respiratory metabolism and ROS level of human chondrocytes treated with Dex. Transmission electron microscopy (TEM) showed that mitochondria were enlarged while mitochondrial matrix density and mitochondria number, as well as cristae density, were reduced in chondrocytes treated with 500 nM Dex for 48 h and 72 h compared with that in the control group; however, no significance was shown in human chondrocytes treated with Dex for 48 h or 72 h (Fig. 2A-D). Further study showed that the higher concentration of Dex (500 and 1000 nM) treated for 48 h significantly reduced the expression of mitochondrial encoding genes involved in oxidative phosphorylation and respiration chain (Fig. 2E). In addition, the level of mtDNA copy number was also significantly reduced in chondrocytes treated with 500 and 1000 nM Dex (Fig. 2F). Moreover, the ratio between JC-1 aggregates and JC-1 monomers was remarkably decreased as the Dex concentration increased, which indicated lower ΔΨm (Fig. 2G, H). At last, the DCFH-DA probe demonstrated that the Dex concentration over 250 nM increased the ROS level of chondrocytes (Fig. 2I, J). Taken together, these results suggested that Dex led to mitochondrial dysfunction and increased levels of ROS.

3.3. Dex caused LA accumulation in chondrocytes via downregulating the level of MCT4

Next, we examined whether the process of glycolysis was enhanced compensatively owing to impaired mitochondrial respiration. The mRNA level of *Hk1*, a mitochondrial enzyme that initiates glycolysis, was obvious reduced in the cartilage of the Dex group, as determined in RT-qPCR (Fig. 3A). However, the mRNA level of *Pfkm* and *Pkm*, involved in glycolysis, showed no significant difference in the cartilage between the two groups (Fig. 3A). Moreover, the mRNA levels of *Hk1* and *Pfkm* were reduced and *Pkm* has a decreasing trend in human chondrocytes treated with Dex (500 and 1000 nM) (Fig. 3B). Meanwhile, we found that with the Dex treatment, the LDH activity in the culture medium of chondrocytes was unchanged but significantly reduced inside the chondrocytes (Fig. 3C, D), which indicated the inhibition of glycolysis. Interestingly, we did not detect a reduction of LA, the product of glycolysis, in chondrocytes. On the contrary, we found that higher level of LA in chondrocytes and a lower level of LA in the medium when treated with Dex (500 and 1000 nM) (Fig. 3E, F). Therefore, we speculated whether the expression of *Mct1* and *Mct4*, which play key roles in LA excretion, was abnormal. Our result showed that Dex significantly decreased the mRNA expression of *Mct4* in the cartilage while had no influence on the level of *Mct1*, as evident from RT-qPCR results (Fig. 3G). Then, IHC analysis also demonstrated that Dex significantly reduced the protein expression of MCT4 in the cartilage (Fig. 3H). Meanwhile, Dex notably downregulated the mRNA level and the protein level of MCT4 in human chondrocytes (Fig. 3I, J). Additionally, we evaluated the effect of LA on chondrocytes. The results demonstrated that in the different time groups, when the LA concentration exceeds 25 mM, LA obviously inhibited the cell viability of chondrocytes, and at the same concentration, there was no significant difference between the LA treatment groups at different times (Supplementary Fig. 1E). Furthermore, we found that overexpressed *Mct4* in human chondrocytes could increase the expression of MCT4 in the Dex group (Fig. 3K, L). In addition, the overexpression of *Mct4* reversed the low protein level of COL2A1 and ACAN induced by Dex (Fig. 3M). Similarly, overexpression of *Mct4* relieved the Dex-induced high level of ROS and the accumulation of LA in chondrocytes (Fig. 3N-P). All these data above clearly indicated that Dex caused LA accumulation in chondrocytes via downregulating the level of MCT4, thereby decreased the matrix synthesis.

3.4. Dex decreased the H3K4me3 level of MCT4 via increased ROS

Then, we explored the potential molecular mechanism underlying the decreased expression of MCT4 in chondrocytes induced by Dex in vitro. The above results suggested that Dex caused increased ROS levels, so we hypothesized that ROS may be related to the expression of *Mct4*. After analyzing the correlation between the ROS level (Fig. 2H) and the *Mct4* mRNA expression (Fig. 3N) that under the treatment of Dex, we found that the ROS level and the expression of *Mct4* were significantly negatively correlated under Dex treatment (Fig. 4A). Also, we found that Dex significantly decreased the *Mct4* expression, whereas NAC, a broadly used antioxidant, ameliorated the Dex effect and enhanced the expression of *Mct4* (Fig. 4B, C). So, how does ROS affect *Mct4*? We investigated patterns of promoter activity markers on MCT4 using Cistrome DB (http://cistrome.org/db/#/), a comprehensive annotated resource of publicly available ChIP-seq and chromatin accessibility data [29]. H3K4me3, H3K4me1, H3K9ac, H3K36m3, and H3K36m2 were identified in gene regulatory sequence of MCT4 in *Homo sapiens*. Similarly, H3K4me3, H3K27ac and H3K36me3 were identified in *Mus musculus*. The peak of H3K4me3 was the highest in gene regulatory sequence in both *Homo sapiens* and *Mus musculus* (Supplementary Fig. 2). As shown in Fig. 4D, the overlapping ChIP-seq peaks for H3K4me3 were found in the upstream region of MCT4 gene in *Homo sapiens*. Besides, studies have pointed out that ROS can regulate gene expression by affecting epigenetic modification, and H3K4m3, as a ROS-sensitive epigenetic mark can be downregulated by ROS [30]. Therefore, we hypothesized that Dex can inhibit the H3K4me3 level of MCT4 via increasing ROS level. Next, using ChIP-PCR, we found the both Dex and H_2O_2 significantly dampened the abundance of H3K4me3 in MCT4 (Fig. 4E), while NAC can reverse these effects of Dex and restore the H3K4me3 level of MCT4 (Fig. 4F). Taken together, the above results indicated that Dex increased ROS level, and the latter further decreased the H3K4me3 level of MCT4.

3.5. α-KG improved the mitochondrial function and matrix synthesis of chondrocytes under Dex treatment

At last, we explored whether α-KG could improve mitochondrial function and matrix synthesis of chondrocytes. IF assay showed that

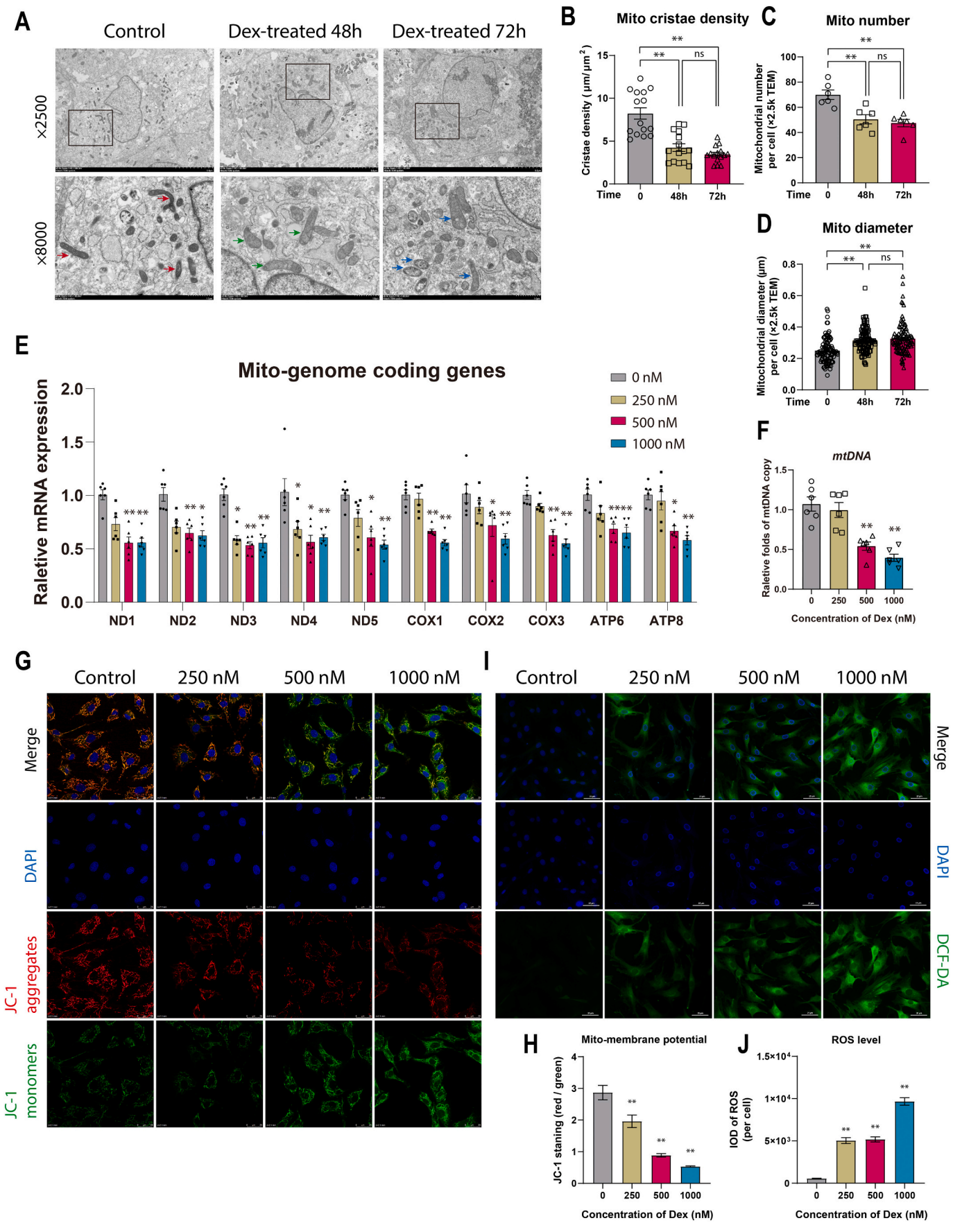

(caption on next page)

Fig. 2. Dex induced chondrocyte mitochondrial dysfunction and increased ROS. (A) The effects of Dex (500 nM) on the mitochondrion of human chondrocytes were analyzed by transmission electron microscopy (TEM). The mitochondrion (Mito) was indicated by red (control), green (48 h), or blue (72 h) arrows. ×2500, ×8000. (B–D) In the TEM images, mitochondrial cristae density, Mito number and Mito diameter were analyzed, $n = 3$. (E) The mRNA expression of mitochondria encoded genes for oxidative phosphorylation and respiration chain in human chondrocytes treated with different concentrations of Dex. Expression was normalized to *Gapdh*, $n = 6$. (F) mtDNA copy number in human chondrocytes treated with different concentrations of Dex. Amplification of mitochondrial gene *ND1* was standardized to 18S rRNA, $n = 6$. (G, H) Representative JC-1 images in human chondrocytes treated with different concentrations of Dex, and the ratio of red and green staining of JC-1. (I, J) DCFH-DA staining images of human chondrocytes treated with different concentrations of Dex and the quantification of the integrated optical density (IOD) per cell, ×400, $n = 6$. The values are the means ± S.E.M.. One-way Anova with Turkey's post hoc tests was used for statistical analysis. $^{*}P < 0.05$, $^{**}P < 0.01$ vs. control. (For interpretation of the references to colour in this figure legend, the reader is referred to the web version of this article.)

α-KG could increase the low level of MCT4 induced by Dex (Fig. 5A, B). Moreover, the ChIP assay indicated that α-KG alleviated the decreased H3K4me3 level induced by Dex (Fig. 5C). In addition, α-KG reduced the ROS level induced by Dex, as determined by RT-qPCR (Fig. 5D, E). Meanwhile, the ratio between JC-1 aggregates and the JC-1 monomers decreased in response to Dex, and α-KG partially reversed the above performance (Fig. 5F, G). Furthermore, Safranin O staining showed α-KG alleviated the ECM loss induced by Dex (Fig. 5H, I). Also, α-KG increased the expression of *Col2a1* and aggrecan and reduced the level of *Mmp13*, as shown in RT-qPCR (Fig. 5J-L). Taken together, α-KG increased the expression of MCT4 and its H3K4me3 level, and improved mitochondrial function and matrix synthesis of chondrocytes under Dex treatment.

4. Discussion

The present study showed that local application of Dex led to chondrocyte matrix synthesis obstacle and the damage of cartilage, which attributed to the high level of ROS and the aberrant accumulation of LA. Mechanismly, the low expression of MCT4 and its decreased H3K4me3 induced by the increased ROS caused LA accumulation. Also, we verified the positive function of α-KG on alleviating the adverse effects of Dex on human chondrocytes.

Relative expression of catabolic and anabolic factors in the cartilage varies to maintain cartilage homeostasis [9]. The disturbance of the balance, such as stronger catabolism proceeds cartilage degradation [31]. Similarly, the normal collagen synthesis function also determines the quality of cartilage [32]. Therefore, factors that affect the synthesis or catabolism of the chondrocyte matrix may affect its normal function. GCs are a class of drugs commonly used for the replacement treatment of acute and chronic adrenal insufficiency [33], the treatment of autoimmune diseases such as rheumatoid arthritis [34], and systemic lupus erythematosus [35], etc. In addition, there are many cases of long-term intra-articular injection of steroids to treat joint diseases [7,36]. However, hormone drugs are a double-edged sword. While they play an active role in treatment, the side effects of long-term systemic or topical application have also become a headache for doctors [37,38]. It is reported that long-term use of GCs increased the risk of femoral head necrosis [39,40]. Dex is one of the representatives of hormone drugs, and it has recently been demonstrated to reduce cartilage inflammation and rescue cartilage matrix loss, suggesting the possibility of Dex as an efficient drug for OA [41,42]. However, Dex can also harm the cartilage. It has been reported that even low doses of Dex caused cell death and reduced cell proliferation, signifying potential cytotoxic and catabolic side effects [43,44]. In the present study, in order to simulate the long-term clinical application of IA GCs as much as possible, we established an IA Dex rat model based on previous studies [21,41], and we found that IA Dex downregulated the expression of cartilage ECM-synthetic *Col2a1* and *Acan* and decreased the matrix content, shown as damaged cartilage. Also, Dex mildly promoted the senescence of chondrocytes in vitro. All these results indicated the cytotoxic effects of Dex on cartilage. It is necessary to state that the IA dose of Dex and its regimen in this study was excessive compared with the clinic in most cases, which aimed to be chosen to demonstrate the potential hazard of Dex to cartilage if used excessively in the clinic.

Mitochondria are remarkably dynamic organelles, which are considered the "powerhouse" of eukaryote cells [45]. Also, mitochondria are significant metabolic centers in chondrocytes and contribute to cellular energy, metabolism, and survival [46,47]. For example, mitochondria generate the energy required for cellular metabolism by OXPHOS [48]. Besides, other intermediate metabolites for bioenergetic metabolism, the redox state, and aging-related responses occur in the mitochondria [45,49]. Mitochondrial dysfunction can cause a surge in ROS levels in cells, triggering a series of cellular stress events and inducing cell death and degeneration [50,51]. It has been demonstrated that Dex was associated with increased oxidative stress [52] and strongly sensitized cells to oxidative stress [53]. Similar to the previous studies above, we also found that Dex increased mitochondrial dysfunction of chondrocytes, including mitochondrial morphology change, reduced mtDNA expression level and $\Delta\Psi m$, and enhanced ROS. These observations verified the adverse effect of Dex on mitochondria of chondrocyte. And upregulation of ROS may account for chondrocyte senescence induced by Dex [54].

Chondrocyte metabolism undergoes dynamic changes in response to different stress conditions [55,56]. In chondrocytes, glycolysis and mitochondrial oxidation work together to maintain the energy metabolism homeostasis [57]. Several lines of evidence suggested that under conditions of environmental stress, chondrocytes tend to adapt their metabolism to microenvironmental changes by shifting from one metabolic pathway to another, for example from oxidative phosphorylation to glycolysis [2]. In this paper, we saw increased ROS and impaired mitochondrial respiration, and further explored the status of glycolysis in the cartilage. However. we failed to see the compensatory enhancement of glycolysis after the treatment of Dex. The expression of the three major rate-limiting enzymes of glycolysis was not increased, and some even were downregulated, which was consistent with the previous researches [9,58]. It is worth noting that some genes are not completely consistent in vivo and in vitro, which may be related to the different metabolic environment and the difference in hormone sensitivity between human and animal chondrocytes. Interestingly, we found high levels of LA (the products of glycolysis) inside the cells, although the glycolysis was inhibited by Dex. It is showed that LA accumulation and the development of a more acidic microenvironment can inhibit matrix synthesis in chondrocytes [2]. Our present results verified this viewpoint. Meanwhile, we found that the expression of MCT4, a lactate transporter to excrete LA out of the cell, was reduced by Dex, while overexpression of MCT4 could reverse the accumulation of LA, the increase of ROS and the damage of matrix synthesis induced by Dex. All these results indicated that Dex inhibited mitochondrial respiration and glycolysis, and decreased the expression of MCT4, which subsequently led to LA accumulation and the damage of chondrocytes.

The change of epigenomes could induce and maintain phenotypic variations in cells and organisms without changing the underlying DNA sequence [59]. GCs are recognized as one of the regulators of epigenetic modification. While its effects on gene expression can persist after the removal, indicating the lasting effects of GCs action and the connections with epigenetics [60,61]. Histone methylations, as a crucial part of epigenetics, are well studied for their roles in the regulation of gene expression and are important post-transcriptional modifications [62,63]. H3K4me3 is an evolutionarily conserved histone modification that marks active transcription and is highly enriched at the promoter region and transcription start site [64,65]. Recently, ROS was reported

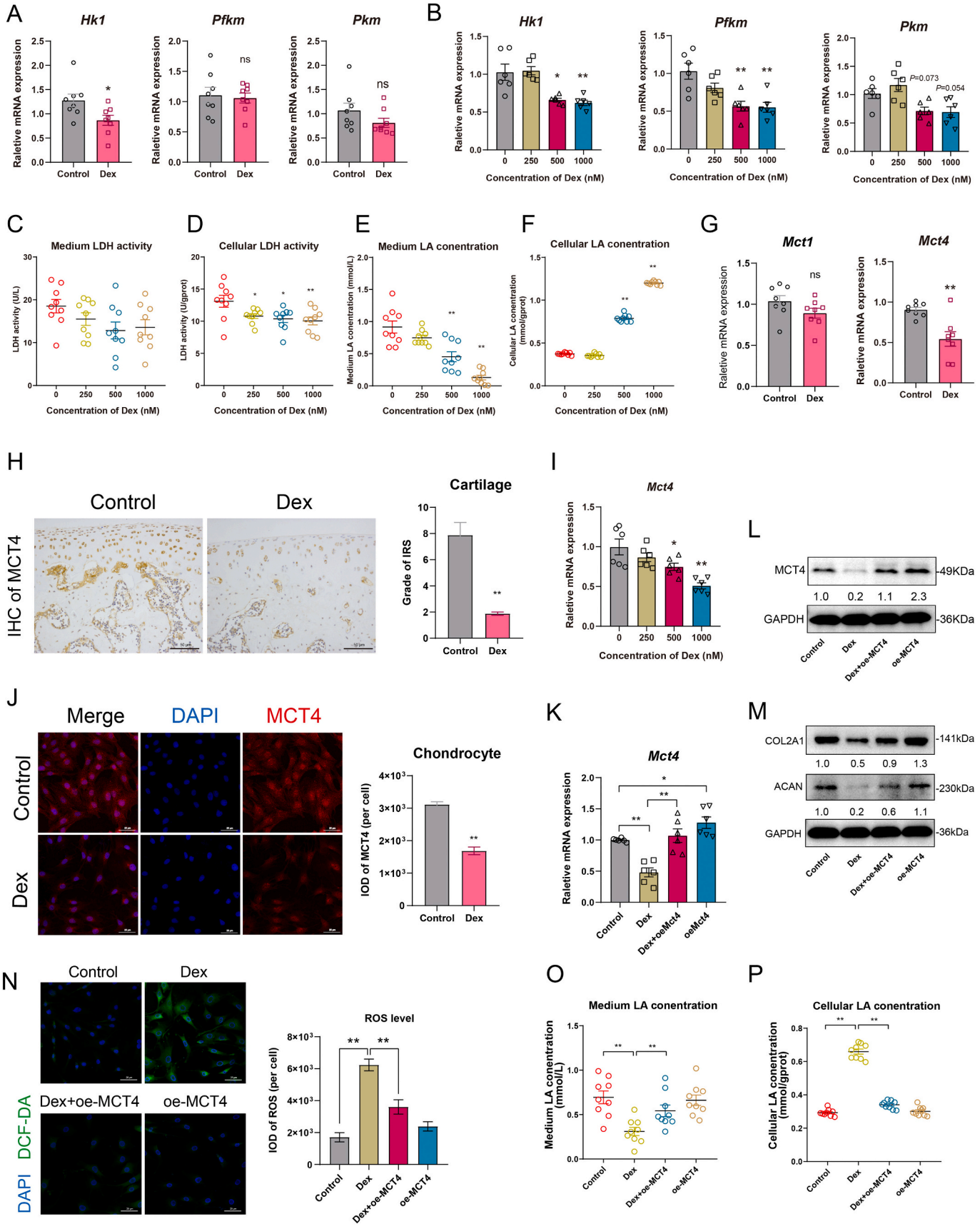

(caption on next page)

Fig. 3. Dex inhibited the expression of MCT4 in chondrocytes and promoted the accumulation of lactic acid (LA). (A) The mRNA expression of hexokinase 1 (*Hk1*), phosphofructokinase (*Pfkm*), pyruvate kinase (*Pkm*) in the rats' cartilage, $n = 8$. (B) The mRNA expression of *Hk1*, *Pfkm,* and *Pkm* in the human chondrocytes treated with different concentrations of Dex, $n = 6$. (C, D) The lactate dehydrogenase (LDH) activity in the medium and in the chondrocyte after the treatment of different concentrations of Dex, $n = 9$. (E, F) The lactic acid (LA) concentration in the medium and in the chondrocyte after the treatment of different concentrations of Dex, n = 9. (G) The mRNA expression of monocarboxylate transporter 1 (*Mct1*) and *Mct4* in the rats' cartilage, n = 8. (H) Representative immunohistochemical images of MCT4 and its quantification (grade of IRS) of the rats' cartilage, ×200, n = 8. (I) The mRNA expression of *Mct4* in the chondrocyte treated with different concentrations of Dex, $n = 6$. (J) Cellular immunofluorescence staining of MCT4 expression after 500 nM Dex treatment and the integrated optical density (IOD) value (per cell) of MCT4, ×400, n = 6. (K) The mRNA level of *Mct4* after the overexpression of *Mct4* in human chondrocytes, n = 6. (L, M) The protein level of MCT4, COL2A1 and ACAN after the overexpression of *Mct4* in human chondrocytes, $n = 3$. (N–P) The level of ROS (n = 6) and LA concentration in the medium and in the chondrocyte (n = 9) after the overexpression of *Mct4* in human chondrocytes. The values are the means ± S.E.M. Mann-Whitney *U* test was used for (A, G, H, J) statistical analysis. One-way Anova with Turkey's post hoc tests was used for comparing multiple groups. $^{*}P < 0.05$, $^{**}P < 0.01$ vs. control.

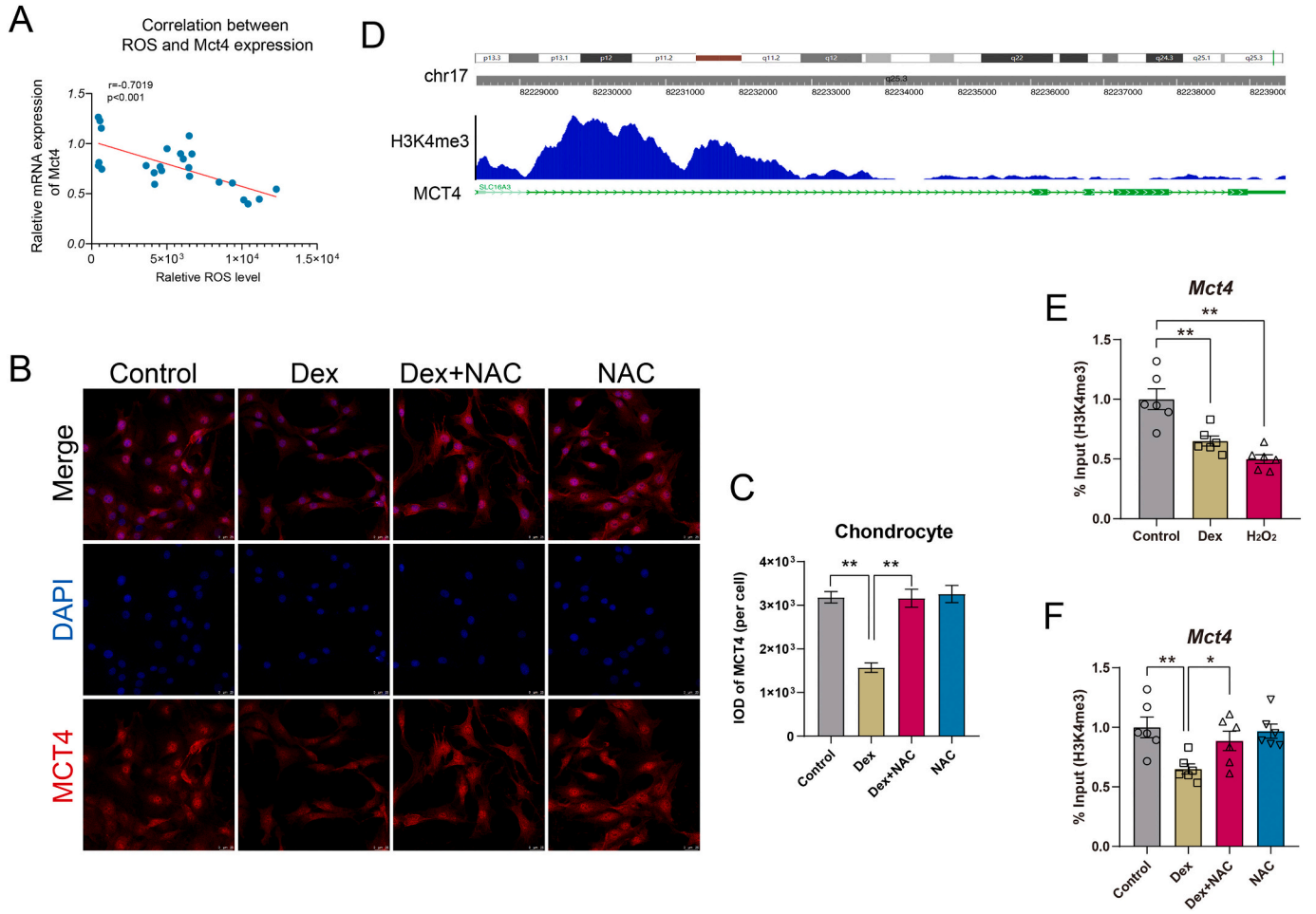

Fig. 4. Dex causes epigenetic changes in MCT4 through ROS. (A) The correlation of ROS level (Fig. 2J) and the mRNA expression of *Mct4* (Fig. 3I). (B, C) Cellular immunofluorescence staining of MCT4 expression after 500 nM Dex, 500 nM Dex combined with 0.5 mM NAC, and 0.5 mM NAC treatment, and the quantification of the integrated optical density (IOD) value (per cell) of MCT4, ×400, $n = 6$. (D) Tracks of H3K4me3 ChIP-seq occupancy in chondrocyte based on data from the Cistrome DB database. (E) The level of H3K4me3 in the promoter region of *Mct4* was assayed by ChIP under the treatment of 500 nM Dex or 100 μM H_2O_2 for 48 h, $n = 6$. (F) The level of H3K4me3 in the promoter region of *Mct4* was assayed by ChIP under the treatment of 500 nM Dex, 500 nM Dex combined with 0.5 mM NAC, and 0.5 mM NAC treatment, n = 6. The values are the means ± S.E.M. Pearson correlation coefficient was used for (A). One-way Anova with Turkey's post hoc tests was used for (C, E, F) statistical analysis. $^{*}P < 0.05$, $^{**}P < 0.01$ vs. control.

to play an important role in modulating the epigenetic landscape under different conditions [66–69], and H3K4m3, as a ROS-sensitive epigenetic mark, could be downregulated by ROS [30]. In the present study, the expression of MCT4 was identified to be negatively correlated with increased ROS. Further study showed that increased ROS reduced the H3K4me3 level and the expression of MCT4 induced by Dex. We proposed that Dex-induced high level of ROS mediated the decreased expression of MCT4 via reducing the level of its H3K4me3 modification, and the epigenetic reprogramming of MCT4 may account for the long-term harmful effects of Dex on cartilage [70,71].

α-KG is an important intermediate of the Krebs cycle and exhibits a crucial role in multiple metabolic processes [72]. Also, some studies suggested α-KG could act as an antioxidant by directly reacting with hydrogen peroxide and could reduce the level of ROS [73–75], and it is recommended as a new strategy for the prevention and treatment of aging and age-related diseases [76]. In the present study, we found that α-KG significantly reduced the level of ROS and ameliorate mitochondrial damage, which played a role similar to antioxidants. In addition, the expression of MCT4 and the level of H3K4me3 were increased after the application of α-KG. Furthermore, α-KG could alleviate the

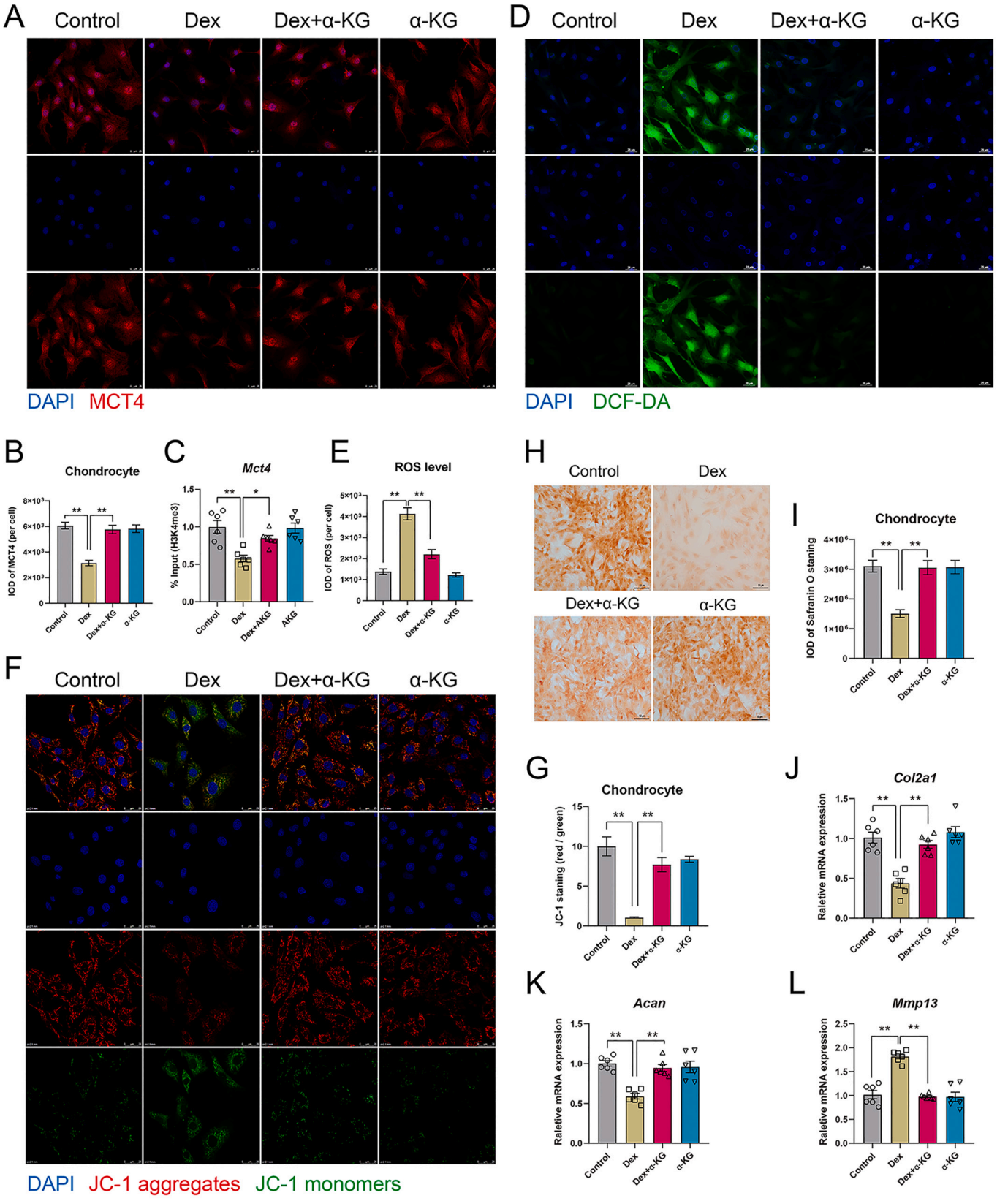

(caption on next page)

Fig. 5. α-KG can alleviate the adverse effects of Dex on cartilage. (A, B) Cellular immunofluorescence staining of MCT4 in human chondrocytes treated with 500 nM Dex, 500 nM Dex combined with 0.5 mM α-KG, and 0.5 mM α-KG treatment, and the quantification of the integrated optical density (IOD) value of MCT4 (per cell), ×400, n = 6. (C) The level of H3K4me3 in the promoter region of *Mct4* was assayed by ChIP under the treatment of 500 nM Dex, 500 nM Dex combined with 0.5 mM α-KG, and 0.5 mM α-KG, n = 6. (D, E) Representative DCFH-DA staining images of human chondrocytes treated with 500 nM Dex, 500 nM Dex combined with 0.5 mM α-KG, and 0.5 mM α-KG, and its IOD value (per cell), ×400, n = 6. (F, G) Representative JC-1 staining images of human chondrocytes treated with 500 nM Dex, 500 nM Dex combined with 0.5 mM α-KG, and 0.5 mM α-KG, and the ratio of red and green staining of JC-1, ×400, n = 6. (H, I) Representative safranin O staining images of human chondrocyte treated with 500 nM Dex, 500 nM Dex combined with 0.5 mM α-KG, and 0.5 mM α-KG, and its IOD value, ×400, n = 6. (J-L) The mRNA expression of *Col2a1, Acan, and Mmp13* in chondrocytes treated with 500 nM Dex, 500 nM Dex combined with 0.5 mM α-KG, and 0.5 mM α-KG, n = 6. The values are the means ± S.E.M. One-way Anova with Turkey's post hoc tests was used for statistical analysis. $*P < 0.05$, $**P < 0.01$ vs. control. (For interpretation of the references to colour in this figure legend, the reader is referred to the web version of this article.)

inhibition of chondrocyte matrix synthesis induced by Dex. In our mind, α-KG may be used as an antioxidant together with Dex to reduce the long-term adverse effects of Dex on cartilage. However, when combined with Dex, the antioxidant effect of α-KG in vivo needs to be further studied.

There are still some limitations in this study. First, NAC and α-KG were demonstrated to reduce ROS level and alleviate the inhibition of chondrocyte matrix synthesis induced by Dex in in vitro experiments, but their effect in vivo requires further confirmation. Second, only male rats were included in this study, and whether there is a gender difference in the adverse effects of Dex on cartilage is still unknown. In the future research, we need to pay more attention to the sensitivity of different genders to Dex therapy, in order to guide clinical practice more pertinently.

In conclusion, this study put forward a new mechanism of the adverse effect of Dex on chondrocytes. Dex exhibited harm to cartilage via mitochondrial dysfunction and increased ROS, the latter mediated the decrease of H3K4me3 level and expression of MCT4, thereby caused the accumulation of intracellular LA, which might also account for the long-term side effects of Dex on chondrocytes. Also, This study proposes a remedy scheme when using Dex, which may guide the clinical application of Dex.

CRediT authorship contribution statement

Qingxian Li: Conceptualization, Investigation, Formal analysis, Writing – review & editing, Validation. **Haitao Chen:** Conceptualization, Investigation, Formal analysis, Writing – review & editing, Validation. **Zhenyu Li:** Formal analysis, Validation. **Fan Zhang:** Formal analysis, Validation. **Liaobin Chen:** Conceptualization, Validation.

Declaration of competing interest

All of the authors state that they have no conflicts of interest.

Acknowledgments

We would like to thank Prof. Biao Chen for his contribution to the acquisition of human specimens in this study. And thanks for the grants from the Guangxi Natural Science Foundation youth Project (No. 2018GXNSFBA281117) owned by Luo Hanwen which supported part of the experiments in this study.

Appendix A. Supplementary data

Supplementary data to this article can be found online at https://doi.org/10.1016/j.bone.2021.116299.

References

[1] M.C. Chang, P.F. Chiang, Y.J. Kuo, C.L. Peng, K.Y. Chen, Y.C. Chiang, Hyaluronan-loaded liposomal dexamethasone-diclofenac nanoparticles for local osteoarthritis treatment, Int. J. Mol. Sci. 22 (2) (2021).
[2] L. Zheng, Z. Zhang, P. Sheng, A. Mobasheri, The role of metabolism in chondrocyte dysfunction and the progression of osteoarthritis, Ageing Res. Rev. 66 (2021), 101249.
[3] S. Glyn-Jones, A.J. Palmer, R. Agricola, A.J. Price, T.L. Vincent, H. Weinans, A. J. Carr, Osteoarthritis, Lancet 386 (9991) (2015) 376–387.
[4] R.R. Bannuru, M.C. Osani, E.E. Vaysbrot, N.K. Arden, K. Bennell, S.M.A. Bierma-Zeinstra, V.B. Kraus, L.S. Lohmander, J.H. Abbott, M. Bhandari, F.J. Blanco, R. Espinosa, I.K. Haugen, J. Lin, L.A. Mandl, E. Moilanen, N. Nakamura, L. Snyder-Mackler, T. Trojian, M. Underwood, T.E. McAlindon, OARSI guidelines for the non-surgical management of knee, hip, and polyarticular osteoarthritis, Osteoarthr. Cartil. 27 (11) (2019) 1578–1589.
[5] J.A. Block, D. Cherny, Management of Knee Osteoarthritis: what internists need to know, Med. Clin. North Am. 105 (2) (2021) 367–385.
[6] D.S. Jevsevar, P.B. Shores, K. Mullen, D.M. Schulte, G.A. Brown, D.S. Cummins, Mixed treatment comparisons for nonsurgical treatment of knee osteoarthritis: a network meta-analysis, J. Am. Acad. Orthop. Surg. 26 (9) (2018) 325–336.
[7] T.E. McAlindon, M.P. LaValley, W.F. Harvey, L.L. Price, J.B. Driban, M. Zhang, R. J. Ward, Effect of intra-articular triamcinolone vs saline on knee cartilage volume and pain in patients with knee osteoarthritis: a randomized clinical trial, JAMA 317 (19) (2017) 1967–1975.
[8] C. Zeng, N.E. Lane, D.J. Hunter, J. Wei, H.K. Choi, T.E. McAlindon, H. Li, N. Lu, G. Lei, Y. Zhang, Intra-articular corticosteroids and the risk of knee osteoarthritis progression: results from the osteoarthritis initiative, Osteoarthr. Cartil. 27 (6) (2019) 855–862.
[9] A. Pemmari, T. Leppänen, M. Hämäläinen, T. Moilanen, K. Vuolteenaho, E. Moilanen, Widespread regulation of gene expression by glucocorticoids in chondrocytes from patients with osteoarthritis as determined by RNA-seq, Arthritis Res. Ther. 22 (1) (2020) 271.
[10] J.A.W. Polderman, V. Farhang-Razi, S. van Dieren, P. Kranke, J.H. DeVries, M. W. Hollmann, B. Preckel, J. Hermanides, Adverse side-effects of dexamethasone in surgical patients - an abridged Cochrane systematic review, Anaesthesia 74 (7) (2019) 929–939.
[11] Y. Tu, H. Xue, W. Francis, A.P. Davies, I. Pallister, V. Kanamarlapudi, Z. Xia, Lactoferrin inhibits dexamethasone-induced chondrocyte impairment from osteoarthritic cartilage through up-regulation of extracellular signal-regulated kinase 1/2 and suppression of FASL, FAS, and caspase 3, Biochem. Biophys. Res. Commun. 441 (1) (2013) 249–255.
[12] P. Juni, R. Hari, A.W. Rutjes, R. Fischer, M.G. Silletta, S. Reichenbach, B.R. da Costa, Intra-articular corticosteroid for knee osteoarthritis, Cochrane Database Syst. Rev. (10) (2015), CD005328.
[13] C. Wernecke, H.J. Braun, J.L. Dragoo, The effect of intra-articular corticosteroids on articular cartilage: a systematic review, Orthop. J. Sports Med. 3 (5) (2015), 2325967115581163.
[14] R. Terkeltaub, K. Johnson, A. Murphy, S. Ghosh, Invited review: the mitochondrion in osteoarthritis, Mitochondrion 1 (4) (2002) 301–319.
[15] A.N. Murphy, G. Fiskum, M.F. Beal, Mitochondria in neurodegeneration: bioenergetic function in cell life and death, J. Cereb. Blood Flow Metab. 19 (3) (1999) 231–245.
[16] R.B. Lee, J.P. Urban, Evidence for a negative Pasteur effect in articular cartilage, Biochem. J. 321 (Pt 1) (1997) 95–102 (Pt 1).
[17] K. Johnson, A. Jung, A. Murphy, A. Andreyev, J. Dykens, R. Terkeltaub, Mitochondrial oxidative phosphorylation is a downstream regulator of nitric oxide effects on chondrocyte matrix synthesis and mineralization, Arthritis Rheum. 43 (7) (2000) 1560–1570.
[18] R.S. Lane, Y. Fu, S. Matsuzaki, M. Kinter, K.M. Humphries, T.M. Griffin, Mitochondrial respiration and redox coupling in articular chondrocytes, Arthritis Res. Ther. 17 (1) (2015) 54.
[19] D. Meredith, P. Bell, B. McClure, R. Wilkins, Functional and molecular characterisation of lactic acid transport in bovine articular chondrocytes, Cell. Physiol. Biochem. 12 (4) (2002) 227–234.
[20] N. Yang, H. Wang, W. Zhang, H. Sun, M. Li, Y. Xu, L. Huang, D. Geng, Integrated analysis of transcriptome and proteome to explore the genes related to steroid-induced femoral head necrosis, Exp. Cell Res. 401 (1) (2021), 112513.
[21] Q.X. Li, Z.Y. Li, L. Liu, Q.B. Ni, X. Yang, B. Chen, L.B. Chen, Dexamethasone causes calcium deposition and degeneration in human anterior cruciate ligament cells through endoplasmic reticulum stress, Biochem. Pharmacol. 175 (2020), 113918.
[22] A. Stein, A. Yassouridis, C. Szopko, K. Helmke, C. Stein, Intraarticular morphine versus dexamethasone in chronic arthritis, Pain 83 (3) (1999) 525–532.
[23] M. Ikeuchi, Y. Kamimoto, M. Izumi, K. Fukunaga, K. Aso, N. Sugimura, M. Yokoyama, T. Tani, Effects of dexamethasone on local infiltration analgesia in total knee arthroplasty: a randomized controlled trial, Knee Surg. Sports Traumatol. Arthrosc. 22 (7) (2014) 1638–1643.
[24] A.J. Grodzinsky, Y. Wang, S. Kakar, M.S. Vrahas, C.H. Evans, Intra-articular dexamethasone to inhibit the development of post-traumatic osteoarthritis, J. Orthop. Res. 35 (3) (2017) 406–411.

[25] K. Foote, J. Reinhold, E.P.K. Yu, N.L. Figg, A. Finigan, M.P. Murphy, M.R. Bennett, Restoring mitochondrial DNA copy number preserves mitochondrial function and delays vascular aging in mice, Aging Cell 17 (4) (2018), e12773.
[26] L. Qing-Xian, W. Lin-Long, W. Yi-Zhong, L. Liang, H. Hui, C. Liao-Bin, W. Hui, Programming changes in GLUT1 mediated the accumulation of AGEs and matrix degradation in the articular cartilage of female adult rats after prenatal caffeine exposure, Pharmacol. Res. 151 (2020), 104555.
[27] D. Liang, W.J. Lin, M. Ren, J. Qiu, C. Yang, X. Wang, N. Li, T. Zeng, K. Sun, L. You, L. Yan, W. Wang, m(6)A reader YTHDC1 modulates autophagy by targeting SQSTM1 in diabetic skin, Autophagy (2021) 1–20.
[28] Y.Z. Wang, Q.X. Li, D.M. Zhang, L.B. Chen, H. Wang, Ryanodine receptor 1 mediated dexamethasone-induced chondrodysplasia in fetal rats, Biochim. Biophys. Acta, Mol. Cell Res. 1867 (10) (2020), 118791.
[29] S. Mei, Q. Qin, Q. Wu, H. Sun, R. Zheng, C. Zang, M. Zhu, J. Wu, X. Shi, L. Taing, T. Liu, M. Brown, C.A. Meyer, X.S. Liu, Cistrome data browser: a data portal for ChIP-seq and chromatin accessibility data in human and mouse, Nucleic Acids Res. 45 (D1) (2017) D658–D662.
[30] D. Bazopoulou, D. Knoefler, Y. Zheng, K. Ulrich, B.J. Oleson, L. Xie, M. Kim, A. Kaufmann, Y.T. Lee, Y. Dou, Y. Chen, S. Quan, U. Jakob, Developmental ROS individualizes organismal stress resistance and lifespan, Nature 576 (7786) (2019) 301–305.
[31] Y. Krishnan, A.J. Grodzinsky, Cartilage diseases, Matrix Biol. 71–72 (2018) 51–69.
[32] S. Stegen, G. Rinaldi, S. Loopmans, I. Stockmans, K. Moermans, B. Thienpont, S. M. Fendt, P. Carmeliet, G. Carmeliet, Glutamine Metabolism Controls Chondrocyte Identity and Function, Dev. Cell 53 (5) (2020) 530–544, e8.
[33] E.S. Husebye, B. Allolio, W. Arlt, K. Badenhoop, S. Bensing, C. Betterle, A. Falorni, E.H. Gan, A.L. Hulting, A. Kasperlik-Zaluska, O. Kampe, K. Lovas, G. Meyer, S. H. Pearce, Consensus statement on the diagnosis, treatment and follow-up of patients with primary adrenal insufficiency, J. Intern. Med. 275 (2) (2014) 104–115.
[34] J.A. Sparks, Rheumatoid arthritis, Ann. Intern. Med. 170 (1) (2019). ITC1-ITC16.
[35] D.J. Wallace, E.M. Ginzler, J.T. Merrill, R.A. Furie, W. Stohl, W.W. Chatham, A. Weinstein, J.D. McKay, W.J. McCune, M. Petri, J. Fettiplace, D.A. Roth, B. Ji, A. Heath, Safety and efficacy of belimumab plus standard therapy for up to thirteen years in patients with systemic lupus erythematosus, Arthritis Rheumatol. 71 (7) (2019) 1125–1134.
[36] J.P. Raynauld, C. Buckland-Wright, R. Ward, D. Choquette, B. Haraoui, J. Martel-Pelletier, I. Uthman, V. Khy, J.L. Tremblay, C. Bertrand, J.P. Pelletier, Safety and efficacy of long-term intraarticular steroid injections in osteoarthritis of the knee: a randomized, double-blind, placebo-controlled trial, Arthritis Rheum. 48 (2) (2003) 370–377.
[37] C.R. Kapadia, T.D. Nebesio, S.E. Myers, S. Willi, B.S. Miller, D.B. Allen, E. Jacobson-Dickman, S. Drugs, Therapeutics Committee of the pediatric endocrine, endocrine effects of inhaled corticosteroids in children, JAMA Pediatr. 170 (2) (2016) 163–170.
[38] U.R. Hengge, T. Ruzicka, R.A. Schwartz, M.J. Cork, Adverse effects of topical glucocorticosteroids, J. Am. Acad. Dermatol. 54 (1) (2006) 1–15, quiz 16-8.
[39] R.S. Weinstein, Glucocorticoid-induced osteonecrosis, Endocrine 41 (2) (2012) 183–190.
[40] G. Talamo, E. Angtuaco, R.C. Walker, L. Dong, M.H. Miceli, M. Zangari, G. Tricot, B. Barlogie, E. Anaissie, Avascular necrosis of femoral and/or humeral heads in multiple myeloma: results of a prospective study of patients treated with dexamethasone-based regimens and high-dose chemotherapy, J. Clin. Oncol. 23 (22) (2005) 5217–5223.
[41] R. Black, A.J. Grodzinsky, Dexamethasone: chondroprotective corticosteroid or catabolic killer? Eur. Cell. Mater. 38 (2019) 246–263.
[42] Y. Zhao, C. Wei, X. Chen, J. Liu, Q. Yu, Y. Liu, J. Liu, Drug delivery system based on near-infrared light-responsive molybdenum disulfide nanosheets controls the high-efficiency release of dexamethasone to inhibit inflammation and treat osteoarthritis, ACS Appl. Mater. Interfaces 11 (12) (2019) 11587–11601.
[43] S.C. Manson, R.E. Brown, A. Cerulli, C.F. Vidaurre, The cumulative burden of oral corticosteroid side effects and the economic implications of steroid use, Respir. Med. 103 (7) (2009) 975–994.
[44] N. Bordag, S. Klie, K. Jürchott, J. Vierheller, H. Schiewe, V. Albrecht, J.C. Tonn, C. Schwartz, C. Schichor, J. Selbig, Glucocorticoid (dexamethasone)-induced metabolome changes in healthy males suggest prediction of response and side effects, Sci. Rep. 5 (2015) 15954.
[45] X. Mao, P. Fu, L. Wang, C. Xiang, Mitochondria: potential targets for osteoarthritis, Front. Med. (Lausanne) 7 (2020), 581402.
[46] Y. Chen, Y.Y. Wu, H.B. Si, Y.R. Lu, B. Shen, Mechanistic insights into AMPK-SIRT3 positive feedback loop-mediated chondrocyte mitochondrial quality control in osteoarthritis pathogenesis, Pharmacol. Res. 166 (2021), 105497.
[47] J. Nakhle, A.M. Rodriguez, M.L. Vignais, Multifaceted roles of mitochondrial components and metabolites in metabolic diseases and cancer, Int. J. Mol. Sci. 21 (12) (2020).
[48] B. Zhou, R. Tian, Mitochondrial dysfunction in pathophysiology of heart failure, J. Clin. Invest. 128 (9) (2018) 3716–3726.
[49] A.S. Rambold, E.L. Pearce, Mitochondrial dynamics at the Interface of immune cell metabolism and function, Trends Immunol. 39 (1) (2018) 6–18.
[50] A. Suomalainen, B.J. Battersby, Mitochondrial diseases: the contribution of organelle stress responses to pathology, Nat. Rev. Mol. Cell Biol. 19 (2) (2018) 77–92.
[51] M.T. Lin, M.F. Beal, Mitochondrial dysfunction and oxidative stress in neurodegenerative diseases, Nature 443 (7113) (2006) 787–795.
[52] M. Suntiparpluacha, N. Tammachote, R. Tammachote, Triamcinolone acetonide reduces viability, induces oxidative stress, and alters gene expressions of human chondrocytes, Eur. Rev. Med. Pharmacol. Sci. 20 (23) (2016) 4985–4992.
[53] S.N. Zucker, E.E. Fink, A. Bagati, S. Mannava, A. Bianchi-Smiraglia, P.N. Bogner, J. A. Wawrzyniak, C. Foley, K.I. Leonova, M.J. Grimm, K. Moparthy, Y. Ionov, J. Wang, S. Liu, S. Sexton, E.S. Kandel, A.V. Bakin, Y. Zhang, N. Kaminski, B. H. Segal, M.A. Nikiforov, Nrf2 amplifies oxidative stress via induction of Klf9, Mol. Cell 53 (6) (2014) 916–928.
[54] R.F. Loeser, J.A. Collins, B.O. Diekman, Ageing and the pathogenesis of osteoarthritis, Nat. Rev. Rheumatol. 12 (7) (2016) 412–420.
[55] R.B. Lee, R.J. Wilkins, S. Razaq, J.P. Urban, The effect of mechanical stress on cartilage energy metabolism, Biorheology 39 (1–2) (2002) 133–143.
[56] S.C. Rosa, J. Gonçalves, F. Judas, A. Mobasheri, C. Lopes, A.F. Mendes, Impaired glucose transporter-1 degradation and increased glucose transport and oxidative stress in response to high glucose in chondrocytes from osteoarthritic versus normal human cartilage, Arthritis Res. Ther. 11 (3) (2009), R80.
[57] A. Dalmao-Fernandez, J. Lund, T. Hermida-Gomez, M.E. Vazquez-Mosquera, I. Rego-Perez, F.J. Blanco, M. Fernandez-Moreno, Impaired metabolic flexibility in the osteoarthritis process: a study on transmitochondrial cybrids, Cells 9 (4) (2020).
[58] Y. Lu, H. Liu, Y. Bi, H. Yang, Y. Li, J. Wang, Z. Zhang, Y. Wang, C. Li, A. Jia, L. Han, Y. Hu, Y. Zhao, R. Wang, G. Liu, Glucocorticoid receptor promotes the function of myeloid-derived suppressor cells by suppressing HIF1alpha-dependent glycolysis, Cell. Mol. Immunol. 15 (6) (2018) 618–629.
[59] A.D. Goldberg, C.D. Allis, E. Bernstein, Epigenetics: a landscape takes shape, Cell 128 (4) (2007) 635–638.
[60] E. Heard, R.A. Martienssen, Transgenerational epigenetic inheritance: myths and mechanisms, Cell 157 (1) (2014) 95–109.
[61] J. Cartier, T. Smith, J.P. Thomson, C.M. Rose, B. Khulan, A. Heger, R.R. Meehan, A. J. Drake, Investigation into the role of the germline epigenome in the transmission of glucocorticoid-programmed effects across generations, Genome Biol. 19 (1) (2018) 50.
[62] T. Kouzarides, Histone methylation in transcriptional control, Curr. Opin. Genet. Dev. 12 (2) (2002) 198–209.
[63] J.C. Black, C. Van Rechem, J.R. Whetstine, Histone lysine methylation dynamics: establishment, regulation, and biological impact, Mol. Cell 48 (4) (2012) 491–507.
[64] A. Shilatifard, The COMPASS family of histone H3K4 methylases: mechanisms of regulation in development and disease pathogenesis, Annu. Rev. Biochem. 81 (2012) 65–95.
[65] T. Zhang, S. Cooper, N. Brockdorff, The interplay of histone modifications - writers that read, EMBO Rep. 16 (11) (2015) 1467–1481.
[66] I. Dimauro, M.P. Paronetto, D. Caporossi, Exercise, redox homeostasis and the epigenetic landscape, Redox Biol. 35 (2020), 101477.
[67] M.S. R, Y. Wang, X. Zhang, H. Cheng, L. Sun, S. He, F. Hao, Redox components: key regulators of epigenetic modifications in plants, Int. J. Mol. Sci. 21 (4) (2020).
[68] T. Kietzmann, A. Petry, A. Shvetsova, J.M. Gerhold, A. Görlach, The epigenetic landscape related to reactive oxygen species formation in the cardiovascular system, Br. J. Pharmacol. 174 (12) (2017) 1533–1554.
[69] W. Xu, X. Zhang, G. Liu, M. Zhu, Y. Wu, Z. Jie, Z. Xie, S. Wang, Q. Ma, S. Fan, X. Fang, Oxidative stress abrogates the degradation of KMT2D to promote degeneration in nucleus pulposus, Biochim. Biophys. Acta Mol. basis Dis. 1866 (10) (2020), 165888.
[70] Y.C. Lien, P.Z. Wang, X.M. Lu, R.A. Simmons, Altered transcription factor binding and gene bivalency in islets of intrauterine growth retarded rats, Cells 9 (6) (2020).
[71] R.J.W. Arts, A. Carvalho, C. La Rocca, C. Palma, F. Rodrigues, R. Silvestre, J. Kleinnijenhuis, E. Lachmandas, L.G. Goncalves, A. Belinha, C. Cunha, M. Oosting, L.A.B. Joosten, G. Matarese, R. van Crevel, M.G. Netea, Immunometabolic pathways in BCG-induced trained immunity, Cell Rep. 17 (10) (2016) 2562–2571.
[72] S. Liu, L. He, K. Yao, The antioxidative function of alpha-ketoglutarate and its applications, Biomed. Res. Int. 2018 (2018), 3408467.
[73] L. He, J. Wu, W. Tang, X. Zhou, Q. Lin, F. Luo, Y. Yin, T. Li, Prevention of oxidative stress by α-ketoglutarate via activation of CAR signaling and modulation of the expression of key antioxidant-associated targets in vivo and in vitro, J. Agric. Food Chem. 66 (43) (2018) 11273–11283.
[74] M.M. Bayliak, H.V. Shmihel, M.P. Lylyk, O.M. Vytvytska, J.M. Storey, K.B. Storey, V.I. Lushchak, Alpha-ketoglutarate attenuates toxic effects of sodium nitroprusside and hydrogen peroxide in drosophila melanogaster, Environ. Toxicol. Pharmacol. 40 (2) (2015) 650–659.
[75] B. Zdzisińska, A. Żurek, M. Kandefer-Szerszeń, Alpha-ketoglutarate as a molecule with pleiotropic activity: well-known and novel possibilities of therapeutic use, Arch. Immunol. Ther. Exp. (Warsz) 65 (1) (2017) 21–36.
[76] R.M. Chin, X. Fu, M.Y. Pai, L. Vergnes, H. Hwang, G. Deng, S. Diep, B. Lomenick, V. S. Meli, G.C. Monsalve, E. Hu, S.A. Whelan, J.X. Wang, G. Jung, G.M. Solis, F. Fazlollahi, C. Kaweeteerawat, A. Quach, M. Nili, A.S. Krall, H.A. Godwin, H. R. Chang, K.F. Faull, F. Guo, M. Jiang, S.A. Trauger, A. Saghatelian, D. Braas, H. R. Christofk, C.F. Clarke, M.A. Teitell, M. Petrascheck, K. Reue, M.E. Jung, A. R. Frand, J. Huang, The metabolite alpha-ketoglutarate extends lifespan by inhibiting ATP synthase and TOR, Nature 510 (7505) (2014) 397–401.